# A STACKED EQUILATERAL TRIANGULAR PATCH ANTENNA WITH SIERPINSKI GASKET FRACTAL FOR WLAN APPLICATIONS

## J. Malik and M. V. Kartikeyan

Millimeter Wave Laboratory
Department of Electronics and Computer Engineering
Indian Institute of Technology, Roorkee 247667, India

**Abstract**—In present work, a microstrip Sierpinski modified and fractalized antenna using multilayer structure to achieve dual band behavior for WLAN applications has been proposed. Due to the space-filling properties of fractal geometry, the proposed antenna is smaller in size than the conventional Euclidean-type. An equilateral triangular patch antenna with Sierpinski Gasket fractal shape has been designed and studied. An electromagnetic coupled stacked structure of two different patches operating at two frequencies (2.4 GHz Bluetooth and 5.8 GHz Wireless LAN) has been designed for dual band WLAN applications.

## 1. INTRODUCTION

In recent years, as the demand of portable systems have increased, low profile systems have drawn much interest for researchers. In making such low profile communication systems, the size of the antenna is critical. Microstrip antennas are very popular due to their properties, such as low profile, low cost, conformability and ease of integration with active devices. To the growing demand of MMIC (monolithic microwave integrated circuits) compatible antennas, patch antennas are good solution. To integrate these antennas in MMIC circuits for wireless communication applications the size of these microstrip antennas should be as small as possible without compromising on their performance. Therefore, many kinds of miniaturization techniques,

such as using high dielectric substrates [1], applying resistive or reactive loading [2], increasing the electrical length of the antenna by optimizing its shape [3], use of notches and short circuits on the patch antenna [4], use of magnetic substrates [5] have been proposed and applied to microstrip patch antennas. Techniques to achieve dual band operation of microstrip antennas are also available [6–9]. The application of fractal geometry to conventional patch antenna structures modifies the shape of the antennas in order to increase its effective electrical length at the same time reducing their overall geometrical size.

Because fractal geometries have two main features in common, space-filling and self-similar properties, fractal shape antenna elements present various advantages like wide bandwidth, multiband [10, 11], and reduced antenna size, among others. Sierpinski fractal geometry exhibits well-known features that have been used to construct miniaturized radiating patches either monopole or dipole antennas. By applying the Sierpinski fractal shape to the antennas, the overall electrical length of the antennas increases and the resonance frequency becomes lower than that of conventional monopole, loop, and patch-type antenna. In the present work, Sierpinski Gasket fractal geometry has been applied to an equilateral triangular microstrip patch antennas to reduce its overall size, and the effectiveness of this technique is verified through experimental investigations. It is found that as the iteration number increases, the resonance frequencies become lower than those of the zero iteration, which represents a conventional equilateral triangular patch. In other words, microstrip patch antennas employing Sierpinski Gasket fractal geometry can operate at a much lower frequency range while maintaining an identical overall antenna size. An electromagnetic coupled stacked structure to operate at two different frequencies (2.4 GHz Bluetooth and 5.8 GHz Wireless LAN) has been designed for dual band WLAN applications.

## 2. ANTENNA GEOMETRY

The antenna configuration of proposed stacked resonator structure is shown in Figure 1. Both resonators are equilateral triangles modified with 2nd iteration Sierpinski Gasket fractal. The substrate used has relative permittivity $\varepsilon_r = 3.38$ and thickness 1.524 mm (60 mil). The size of the substrate used is 60 mm by 60 mm. To calculate resonant frequencies of a simple equilateral triangular patch without any degree
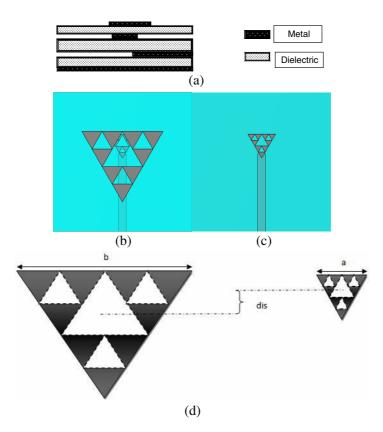
**Figure 1.** (a) Stack antenna configuration. (b) Top view of antenna structure. (c) Top view of bottom patch only. (d) Resonator showed separately (black portion represents metallic part).

of Sierpinski Gasket fractal [12]

$$f_{m,n,1} = \frac{2c}{3a(\varepsilon_r)^{1/2}}(m^2 + mn + n^2)^{1/2} \qquad (1)$$

$$a_{eff} = a + h(\varepsilon_r)^{-1/2} \qquad (2)$$

$$\varepsilon_{eff} = \frac{1}{2}(\varepsilon_r + 1) + \frac{1}{4}(\varepsilon_r - 1)\left(1 + \frac{12h}{a}\right)^{-1/2} \qquad (3)$$

$$f_{m,n} = \frac{2c}{3a_{eff}}(\varepsilon_{eff})^{1/2}(m^2 + mn + n^2)^{1/2} \qquad (4)$$

where

$a$ = length of equilateral triangular patch

$h$ = thickness of substrate

$\varepsilon_r$ = relative dielectric constant

$C$ = velocity of light

$\text{TM}_{m,n}$ is the resonant fundamental mode. Here, $m = 0$ and $n = 1$.

The calculated side length of equilateral triangular patch from above Equations (1)–(4) was taken as starting value. During simulation it was observed that with increase in fractal iteration count the side length for both patch decreased for operation in same band. For 2nd degree fractal bottom patch has side length $a = 11.8\,\text{mm}$ and the upper patch is of side length $b = 35\,\text{mm}$. proximity coupled feed has been used to excite the lower patch and upper patch is electromagnetically coupled to the lower patch. The width of feed line is set to achieve line impedance of 50 ohm. The length of feed line is $33.4\,\text{mm}$ (from lower end of substrate to centroid of upper patch) i.e., the upper end of feed line is just right below the centroid of bigger patch. During simulation, the upper patch kept at fixed location and lower patch moved along $Y$-axis in either direction to achieve higher resonance. The distance between the centers of lower patch and upper patch in $Y$-direction is $5.1\,\text{mm}$. At this tuned position value for parameter "dis" was taken as zero (dis = 0). The center of square patch was at origin and centroids of both the patches were along $Y$-axis.

## 3. RETURN LOSS AND PARAMETRIC VARIATIONS

The proposed antenna was designed and simulated in finite integration technique based CST MWS V9. To simulate the antenna Transient solver was chosen. During simulation Hexahedral mesh cell with 20 Lines per lambda was set up. Far field radiation pattern at two frequency $2.4\,\text{GHz}$ and $5.8\,\text{GHz}$ was selected along with $H$-field/surface current. Port impedance was adjusted to $50\,\Omega$.

The simulated and fabricated return loss results are shown in Figures 2 and 3. The antenna covers the WLAN standards IEEE 802.11 b ($2.4\,\text{GHz}$ band) and IEEE 82.11 a ($5.8\,\text{GHz}$ band). The simulated bandwidth at the $2.4\,\text{GHz}$ band is around $86\,\text{MHz}$ and at the $5.8\,\text{GHz}$ band is around $280\,\text{MHz}$. After fabrication the return loss of the antenna was tested on HP Network Analyzer and the fabricated result was found to be in good agreement with the simulated result.

A detail parametric analysis for the proposed antenna structure was done. From Figure 4, it can be observed that changing the side
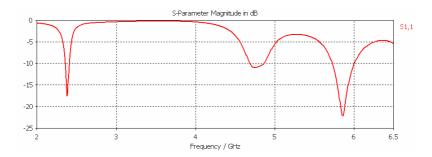
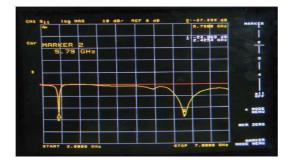**Figure 2.** The simulated return loss of the antenna.



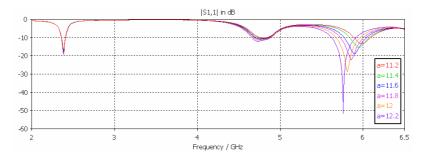**Figure 3.** The measured return loss of the antenna.



**Figure 4.** Effect of varying side length ($a$) of bottom patch on the return loss pattern.

length ($a$) of lower patch has prominent effect on the higher 5.8 GHz band. The resonant frequency decreases as the side length of lower patch increase in 5.8 GHz band which is according to the theory. Changing the side length (a) has no effect on the resonance frequency in 2.4 GHz band except change in magnitude of return loss. From

Figure 5, one can see that the variation of side length of upper patch ($b$) simultaneously affects both 2.4 GHz and 5.8 GHz band resonances, which may be due to EM coupling between the patches. Figure 6 shows the effect of varying the distance between the centroid of patch keeping the upper patch location constant, resonance at 5.8 GHz band changes but has little effect on the resonance at 2.4 GHz band. This distance was varied about tuned position (dis = 0) keeping all other parameter constant (i.e., position of upper patch and size of both patches kept constant during parameter sweep) and changes in return loss was observed. Here tuning is taken in a sense to achieve proper power coupling between the feed-line and the patch which can conveniently be adjusted by changing the parameter "dis" between them. We tuned this parameter to achieve strong coupling between feed and patch. As distance increased in either direction, less coupling occurs between feed line and patch. Again frequency shifting and little change in bandwidth was observed. This is also true for other case, i.e., keeping position of lower patch fixed and by changing 'dis' parameter about tuned value (i.e., shifting upper patch in either direction along $Y$-axis) the 2.4 GHz resonance deteriorates.
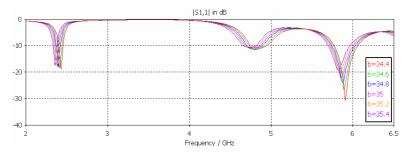


**Figure 5.** Effect of varying side length ($b$) of upper patch on the return loss pattern.
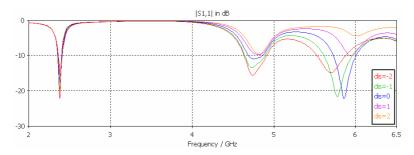


**Figure 6.** Effect of varying distance between the centroid of patches in $Y$-direction on the return loss pattern.

## 4. CURRENT DISTRIBUTION

The current distributions for the lower and upper patches at the 2.4 GHz and 5.8 GHz bands are shown in Figures 7 and 8. As in [6], it can be seen that the current paths have been lengthened because of the introduction fractal on both the patches which leads to an increase in electrical length and hence a decrease in overall patch size.

From Figure 4 it can be observed that at 2.4 GHz current path is larger in upper patch which is quite expected. Similar observations
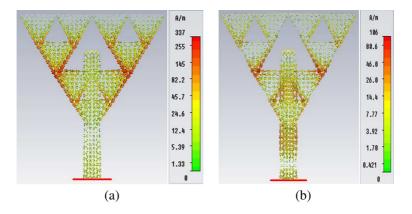


**Figure 7.** Current distributions on upper patch at (a) 2.4 GHz and (b) 5.8 GHz bands.
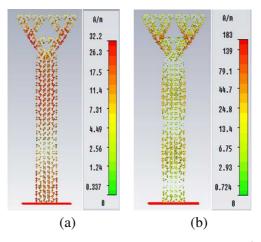


**Figure 8.** Current distributions on lower patch at (a) 2.4 GHz and (b) 5.8 GHz bands.

can be done in case of lower patch at higher resonance. The surface current densities on both the patches are shown for both 2.4 GHz and 5.8 GHz frequencies. From the current density values shown against each patch, it can be concluded that at higher resonance, i.e., 5.8 GHz frequency the current density on smaller patch is more compared to that of bigger patch. That means it is more responsible for higher resonance. Similar results can be concluded for bigger patch from the Figures 7 and 8.

## 5. MEASUREMENT RESULTS

The return loss was measured with HP network analyzer (HP 8720B). The radiation performance has been measured in the anechoic chamber. 15 dBm power was given to the transmitter antenna from the RF power generator, and the distance between the transmitter and the receiver was kept at 1.5 meter. The gain is calculated using substitution method with the help of the Standard Gain Horn antenna (reference antenna) working in the range 0.9 to 8 GHz.

The simulated antenna was fabricated using photolithography process; thereafter its radiation pattern ($E$ field and $H$ field power pattern) was measured. Figure 9 shows the antenna being tested on the network analyzer.



**Figure 9.** The fabricated antenna being tested on network analyzer.

Figures 10 and 11 show the simulated and measured radiation patterns of the antenna in both the $E$-plane and the $H$-plane at the frequency bands of 2.4 GHz and 5.8 GHz. The simulated and measured radiation patterns for $E$-plane at both 2.4 GHz and 5.8 GHz band are in close agreement. The measured radiation pattern in $H$-plane at both 2.4 GHz and 5.8 GHz band are somewhat distorted compared to that of simulated patterns. This may be due to the fact that very low power levels are received by the antenna at 2.4 GHz and 5.8 GHz band in $H$-plane configuration as compared to the other

2 configurations. Possible reasons for these disagreements between simulated and measured results may due to the possible presence of interference and noise.

The simulated and measured gain curves are given for the 2.4 GHz and 5.8 GHz bands in Figure 12. At both 2.4 GHz and 5.8 GHz bands the maximum power was received by the antenna at the broadside direction. Consequently, gain measurements are done for the two frequency bands in the directions of their respective maxima using the substitution/gain-transfer technique with the help of a standard horn antenna with calibrated gain. About 1–1.2 dB of difference in the simulated and measured gains is observed which can be attributed to fabrication and measurement errors.
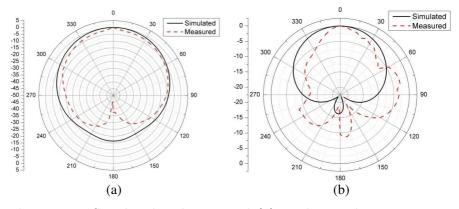


**Figure 10.** Simulated and measured (a) E-plane radiation pattern, (b) H-plane radiation pattern at 2.4 GHz.
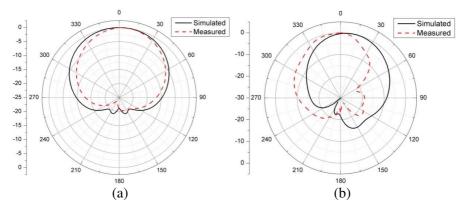


**Figure 11.** Simulated and measured (a) E-plane radiation pattern, (b) H-plane radiation pattern at 5.8 GHz.
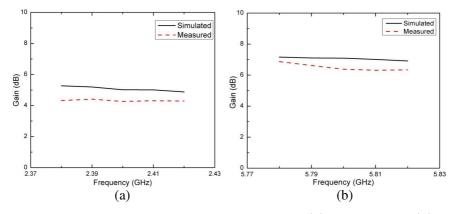
**Figure 12.** Simulated and measured gains at (a) 2.4 GHz and (b) at 5.8 GHz bands.

## 6. CONCLUSIONS

A stacked structure of Sierpinski Gasket fractal geometry applied to an equilateral triangular microstrip patch antenna was designed with fractal shapes being excoriated from both the radiating patch surfaces. The fractal modifications (2nd degree Sierpinski Gasket) resulted in longer current paths on the patches which led to a size reduction. For a simple equilateral triangular patch having zero iteration of Sierpinski gasket fractal, the side length of resonating patch (for $m = 0$, $n = 1$) are $\approx 45.2$ mm and $\approx 18.7$ mm for 2.4 GHz and 5.8 GHz respectively. The side lengths of resonating equilateral triangular patch with 2nd iteration Sierpinski gasket fractal are 35 mm and 11.8 mm for 2.4 GHz and 5.8 GHz respectively. A significant size reduction of about 22% and 36% for 2.4 GHz band and 5.8 GHz band respectively observed in present study. In addition the stack structures make possible simultaneous dual band performance of the antenna. The return loss of the fabricated antenna indicates a $-10$ dB impedance bandwidth of 64 MHz at the 2.4 GHz band and an impedance bandwidth of 500 MHz at the 5.8 GHz band.

## REFERENCES

1. Lo, T. K. and Y. Hwang, "Microstrip antennas of very high permittivity for personal communications," *1997 Asia Pacific Microwave Conference*, 253–256, 1997.

2. Sinati, R. A., *CAD of Microstrip Antennas for Wireless Applications*, Artech House, Norwood, MA, 1996.

3. Wang, H. Y. and M. J. Lancaster, "Aperture coupled thin-film superconducting meander antennas," *IEEE Transaction on Antennas Propagation*, Vol. 47, 829–836, 1999.

4. Waterhouse, R., *Printed Antennas for Wireless Communications*, John Wiley & Sons Inc., 2007.

5. Anguera, J., L. Boada, C. Puente, C. Borja, and J. Soler, "Stacked *H*-shaped microstrip patch antenna," *IEEE Transactions on Antennas and Propagation*, Vol. 52, No. 4, April 2004.

6. Kordzadeh, A. and F. Hojat Kashani, "A new reduced size microstrip patch antenna with fractal shaped defects," *Progress In Electromagnetics Research B*, Vol. 11, 29–37, 2009.

7. Sanad, M. and N. Hassan, "Mobile cellular/GPS/satellite antennas with both single-band and dual-band feed points," *Proc. IEEE Antennas and Propagation Int. Symp.*, Vol. 1, 298–301, Salt Lake City, UT, July 2000.

8. Moleiro, A., J. Rosa, R. Nunes, and C. Peixeiro, "Dual band microstrip patch antenna element with parasitic for GSM," *Proc. IEEE Antennas and Propagation Int. Symp.*, Vol. 4, 2188–2191, Salt Lake City, UT, July 2000.

9. Zhong, S. S. and J. H. Cui, "Compact dual-frequency microstrip antenna," *Proc. IEEE Antennas and Propagation Int. Symp.*, Vol. 4, 2196–2199, Salt Lake City, UT, July 2000.

10. Puente, C., J. Romeu, R. Pous, and A. Cardma, "On the behavior of the Sierpinski multiband fractal antenna," *IEEE Transaction on Antennas Propagation*, Vol. 46, 517–521, 1998.

11. Tiwari, H. and M. V. Kartikeyan, "A stacked microstrip patch antenna with fractal shaped defects," *Progress In Electromagnetic Research C*, Vol. 14, 185–195, July 2010.

12. Dahele, J. S., "On the resonant frequencies of the triangular patch antenna," *IEEE Transactions on Antennas and Propagation*, Vol. 35, No. 1, 100–101, 1987.